THE JOURNAL OF BIOLOGICAL CHEMISTRY
Vol. 279, No. 42, Issue of October 15, pp. 44133–44140, 2004
Printed in U.S.A.

Scanning Mutagenesis of ω-Atracotoxin-Hv1a Reveals a Spatially Restricted Epitope That Confers Selective Activity against Insect Calcium Channels*

Received for publication, April 12, 2004, and in revised form, August 3, 2004
Published, JBC Papers in Press, August 11, 2004, DOI 10.1074/jbc.M404006200

Hugo W. Tedford‡, Nicolas Gilles§, André Ménez§, Clinton J. Doering¶‖, Gerald W. Zamponi¶‖, and Glenn F. King‡**

From the ‡Department of Molecular, Microbial, and Structural Biology, University of Connecticut Health Center, Farmington, Connecticut 06032-3305, §Departement d'Ingenierie et d'Etudes des Proteines, Commissariat a l'Energie Atomique, Saclay, 91191 Gif-sur-Yvette, France, and ¶Department of Physiology & Biophysics, Cellular and Molecular Neurobiology Research Group, University of Calgary, 3330 Hospital Dr. NW, Calgary, Alberta T2N 4N1, Canada

We constructed a complete panel of alanine mutants of the insect-specific calcium channel blocker ω-atracotoxin-Hv1a. Lethality assays using these mutant toxins identified three spatially contiguous residues, Pro^{10}, Asn^{27}, and Arg^{35}, that are critical for insecticidal activity against flies (*Musca domestica*) and crickets (*Acheta domestica*). Competitive binding assays using radiolabeled ω-atracotoxin-Hv1a and neuronal membranes prepared from the heads of American cockroaches (*Periplaneta americana*) confirmed the importance of these three residues for binding of the toxin to target calcium channels presumably expressed in the insect membranes. At concentrations up to 10 μM, ω-atracotoxin-Hv1a had no effect on heterologously expressed rat $Ca_v2.1$, $Ca_v2.2$, and $Ca_v1.2$ calcium channels, consistent with the previously reported insect selectivity of the toxin. 30 μM ω-atracotoxin-Hv1a inhibited rat Ca_v currents by 10–34%, depending on the channel subtype, and this low level of inhibition was essentially unchanged when Asn^{27} and Arg^{35}, which appears to be critical for interaction of the toxin with insect Ca_v channels, were both mutated to alanine. We propose that the spatially contiguous epitope formed by Pro^{10}, Asn^{27}, and Arg^{35} confers specific binding to insect Ca_v channels and is largely responsible for the remarkable phyletic selectivity of ω-atracotoxin-Hv1a. This epitope provides a structural template for rational design of chemical insecticides that selectively target insect Ca_v channels.

The first peptide neurotoxins isolated from the venom of Australian funnel-web spiders (genera *Atrax* and *Hadronyche*) and shown to have selective activity against insects were members of the ω-atracotoxin-1 (ACTX)[1] family (1–3). These toxins comprise 36–37 residues with six strictly conserved cysteine residues that are paired to form three disulfide bridges (4). The best studied family member, ω-ACTX-Hv1a, is one of the most potent insecticidal peptide toxins discovered so far (4, 5); it has proved lethal to all insect orders that have been tested, including coleopterans, dictyopterans, hemipterans, orthopterans, and refractory lepidopteran pests such as the tobacco budworm *Heliothis virescens* and the cotton bollworm *Helicoverpa armigera* (1, 2, 5).

The phyletic specificity of these toxins appears to reside in their ability to block insect, but not vertebrate, voltage-gated calcium channels (2). Although nanomolar concentrations of ω-ACTX-Hv1a are sufficient to block high voltage-activated (HVA) calcium currents in the central nervous system of the fruit fly *Drosophila melanogaster* and the American cockroach *Periplaneta americana* (2, 5), 1 μM toxin does not block HVA calcium currents in vertebrate neurons (2) and the toxin is harmless when injected subcutaneously into newborn mice (1).

With the exception of the organophosphate and carbamate insecticides (which target acetylcholinesterase), the vast majority of synthetic insecticides are directed against voltage-gated sodium channels, nicotinic acetylcholine receptors, or GABA/glutamate-gated chloride channels. This limited group of targets has promoted the evolution of cross-resistance to different families of insecticides (6) and stimulated interest in the development of new insecticides that act on targets outside of this established ion channel triumvirate (7). Although blockers of HVA calcium currents have evolved independently in the venoms of cone snails, snakes, and spiders (4, 8, 9), no commercially available insecticide exploits this target (7, 10). Thus, ω-ACTX-Hv1a is a valuable lead for the development of a new class of insecticides that target insect calcium channels.

The three-dimensional structure of ω-ACTX-Hv1a comprises a disulfide-rich globular core (residues 4–21), with residues 22–37 forming a finger-like β hairpin that protrudes from this globular region (2). In a previous structure-activity relationship study, we demonstrated the functional significance of several residues in the toxin's β hairpin (11). In the present study, we extended our scanning mutagenesis of ω-ACTX-Hv1a in several ways: first, we employed a complete panel of alanine mutations representing all solvent-exposed side chains of the toxin structure; second, we tested these mutations using lethality assays performed in two distantly related insects, the orthopteran *Acheta domestica* and the dipteran *Musca domestica*; third, by performing competitive binding assays using a neuronal membrane preparation from the head of *P. americana*, we obtained information about the toxin-target interaction that is

* This work was supported in part by grants (to G. F. K.) from the National Science Foundation (MCB9983242) and the National Institute of Allergy and Infectious Diseases (1-R41-AI51791) and a grant (to G. W. Z.) from the Heart and Stroke Foundation of Alberta and the Northwest Territories. The costs of publication of this article were defrayed in part by the payment of page charges. This article must therefore be hereby marked "*advertisement*" in accordance with 18 U.S.C. Section 1734 solely to indicate this fact.

‖ Supported by salary awards from the Alberta Heritage Foundation for Medical Research.

** To whom correspondence should be addressed: Dept. of Molecular, Microbial, and Structural Biology, University of Connecticut Health Center, 263 Farmington Ave., Farmington, CT 06032-3305. Tel.: 860-679-8364; Fax: 860-679-1652; E-mail: glenn@psel.uchc.edu.

[1] The abbreviations used are: ACTX, atracotoxin; HVA, high voltage-activated; WT, wild-type; HEK, human embryonic kidney; VGCC, voltage-gated calcium channel; $\Delta\Delta G_{bind}$, change in the free energy of binding.

not complicated by issues of bioavailability and/or pharmacokinetics. The data indicate that a spatially contiguous epitope composed of residues Pro^{10}, Asn^{27}, and Arg^{35} is responsible for the specific interaction of this toxin with insect calcium channels. A panel of follow-up mutants was used to ascertain the key chemical features of these residues that are critical for the toxin-channel interaction. This information should facilitate the rational design of chemical insecticides based on the structure of ω-ACTX-Hv1a.

EXPERIMENTAL PROCEDURES

Production of ω-ACTX-Hv1a Mutants—Individual point mutations were introduced into a synthetic gene encoding ω-ACTX-Hv1a as described previously (11) using either 1) mutagenic PCR using the C2 primer, a mutagenic version of the N1 primer (with pHWT1 as a template), or 2) overlap extension PCR using a pair of complementary mutagenic primers in combination with the original N1 and C2 primers (with pHWT1 as a template). The full-length product of the mutagenic PCR was then digested with EcoRI and BamHI and subcloned into the expression vector pGEX-2T as described previously for pHWT-1 (11). Double mutations were introduced by a similar process in which a version of pHWT-1 encoding one of the two desired mutations was used as the PCR template. Overexpression and purification of recombinant wild-type (WT) ω-ACTX-Hv1a and mutants thereof was performed as described previously using glutathione affinity chromatography followed by C_{18} reverse-phase high pressure liquid chromatography (11). The identity of each toxin was confirmed using electrospray mass spectrometry.

Insect Toxicity Assays—Insecticidal activity was tested as described previously (11, 12) by injecting peptides dissolved in insect saline (13) into house crickets (*Acheta domestica*) or house flies (*Musca domestica*). LD_{50} values (*i.e.* the dose that is lethal to 50% of insects) were calculated as described previously (11), and the reported values are the mean of two to three independent experiments.

CD Spectroscopy—CD spectra of ω-ACTX-Hv1a or mutants thereof were collected and processed as described previously using a Jasco J-715 spectropolarimeter (11). The toxin concentration was 15 μM.

Radiolabeling of Recombinant ω-ACTX-Hv1a—Lethality assays performed with crickets showed that although mutation of Tyr to Phe at residue 13 of ω-ACTX-Hv1a was not deleterious, other mutations at this residue (such as Tyr to Trp or Ala) can lower toxin activity (see "Results"). Hence, Tyr^{13} is not a good target for iodination. Because the initial alanine scan of the β-hairpin region of ω-ACTX-Hv1a (11) revealed that an F24A mutation was tolerated, we decided to engineer a "YF swap mutant," in which Tyr^{13} was mutated to Phe and Phe^{24} was mutated to Tyr, for use as a radioiodination substrate. The swap mutant was fully functional in LD_{50} assays and it contained a single, non-critical Tyr residue (Tyr^{24}) that allowed radioactive iodine to be conjugated to residue 24 rather than to residue 13. Radioiodination of the YF swap mutant was performed as described previously for ω-conotoxin GVIA (14) except for minor changes in the reverse-phase high pressure liquid chromatography method used to purify the radiolabeled toxin. The purification was performed using a Vydac C_{18} analytical reverse-phase column (4.6 × 250 mm; 5 μm pore size) eluted at 1 ml/min using a linear gradient of 0–28% buffer B (0.085% trifluoroacetic acid and 50% acetonitrile in water) in buffer A (0.1% trifluoroacetic acid in water) over 5 min, followed by a linear gradient of 28–35% buffer B in buffer A over 15 min, followed by a linear gradient of 35–53% buffer B in buffer A over 12 min. Cold toxin was observed to elute at 19 min (*i.e.* during the last minute of the second gradient); monoiodinated toxin was observed to elute at 21–22 min. Hereinafter, the radiolabeled swap mutant will be referred to as ^{125}I-ω-ACTX-Hv1a.

Preparation of Cockroach Neuronal Membranes—Neuronal membranes were prepared from the heads of adult *P. americana* as described previously (15), except that the final Ficoll centrifugation step was eliminated. The concentration of membrane proteins in the final preparation was determined using a Bradford protein assay (Bio-Rad) with bovine serum albumin as a standard.

Competitive Binding Assays using Radiolabeled ω-ACTX-Hv1a—Equilibrium competition binding experiments were performed using increasing concentrations of unlabeled mutant toxin in the presence of a fixed concentration of ^{125}I-ω-ACTX-Hv1a. Individual binding reactions were brought to a final volume of 100 μl in binding buffer (75 mM NaCl, 5 mM $CaCl_2$, 50 mM HEPES, and 0.1% bovine serum albumin, pH 7.4). Cockroach neuronal membranes were added to binding reactions to a final concentration of ~0.15 μg of membrane protein/μl. ^{125}I-ω-ACTX-Hv1a was added to a final concentration of 1–1.5 nM. Unlabeled competitors were present at various final concentrations. After incubation at room temperature for 60 min, the reactions were terminated by dilution with 2 ml of ice-cold wash buffer (300 mM choline chloride, 5 mM $CaCl_2$, 50 mM HEPES, and 0.1% bovine serum albumin, pH 7.4). Bound toxin was recovered from the diluted reactions using rapid vacuum filtration through GF/C filters (Whatman) preincubated in 0.3% polyethylenimine (Sigma-Aldrich). The filters were then rapidly washed three times with 2 ml of wash buffer. Nonspecific toxin binding was determined in the presence of 10 μM unlabeled ω-ACTX-Hv1a and typically comprised 40–50% of total binding. Counts of the washed filters were analyzed using KaleidaGraph (Abelbeck/Synergy, Reading, PA) to fit data to a non-linear Hill equation for IC_{50} determination. K_i values were calculated using the Cheng-Prusoff equation (which assumes pure competition at a single site), $K_i = IC_{50}/[1 + (L^*/K_d)]$, where L^* is the concentration of radiolabeled toxin and K_d is its dissociation constant (16). The K_d value used for these computations was obtained by using the computer program LIGAND (Elsevier Biosoft) to perform iterative Scatchard analysis on data from competition binding experiments performed with ^{125}I-ω-ACTX-Hv1a and unlabeled wild-type ω-ACTX-Hv1a.

Patch-clamp Recordings—Human embryonic kidney (HEK) tsA-201 cells were grown and transfected with cDNAs encoding α1, α2-δ, and β subunits of rat HVA calcium channels as described previously (17). Whole-cell patch-clamp recordings were acquired from the transiently transfected tsA-201 cells as described previously (17).

RESULTS

Alanine-scanning Mutagenesis of ω-ACTX-Hv1a—We expanded a collection of described previously alanine mutants of ω-ACTX-Hv1a (11) to give a larger panel of 28 mutants that comprised individual alanine mutations at all positions corresponding to solvent-exposed non-glycine sidechains of the toxin. The six cysteine residues that form the toxin's cystine-knot motif (2, 10) were excluded from the mutational analysis because their side chains are involved in disulfide bonds that are critical to the three-dimensional structure of the toxin. Ile^5 was excluded because it forms part of the buried hydrophobic core of the toxin (2) and is likely to be critical for toxin folding. Gly^8 and Gly^{30} were also excluded because they are located in β-turns that are likely to be structurally important (2). Moreover, with only a hydrogen atom side chain, the Gly residues are unlikely to be functionally important. The P6A and S19A mutant toxins were difficult to overexpress and purify, and were therefore not used in the fly toxicity assays.

Structural Integrity of Mutant Toxins—Although the mutations that we introduced into ω-ACTX-Hv1a were chosen to avoid major structural perturbations, it was important to test this experimentally. We did this by acquiring CD spectra of the WT and mutant recombinant toxins. The CD spectrum of WT toxin exhibits a β sheet signature (Fig. 1*A*) with pronounced minima and maxima at 210 and 196 nm, respectively (11); this is consistent with a 16-residue β hairpin (residues 22–37) being the major secondary structure feature of ω-ACTX-Hv1a (2) (see Fig. 1*C*). The small positive band at 236 nm is presumably caused by the aromatic chromophore of Tyr^{13}, since this feature is absent in CD spectra of Y13A and Y13L mutants but present (albeit slightly blue-shifted) in the spectrum of a Y13W mutant (Fig. 1*B*).

We showed previously that none of the alanine-scan mutants in the β-hairpin region of the toxin were structurally perturbed except for mutations at Lys^{34} (11). Likewise, the CD spectrum of 13 of the 15 newly constructed alanine mutants in the disulfide-rich globular portion of the toxin superimposed closely on the CD spectrum of the WT recombinant toxin, as illustrated for the S1A and Q9A mutants in Fig. 1*A*. Only the CD spectra of the Y13A and N16A mutants differed significantly from that of the WT toxin. The CD spectrum of the Y13A mutant was similar to that of the WT toxin except that the Tyr^{13} side chain signature at 236 nm was absent as expected (Fig. 1*B*). We conclude that the backbone fold of the Y13A mutant is similar to that of the native toxin.

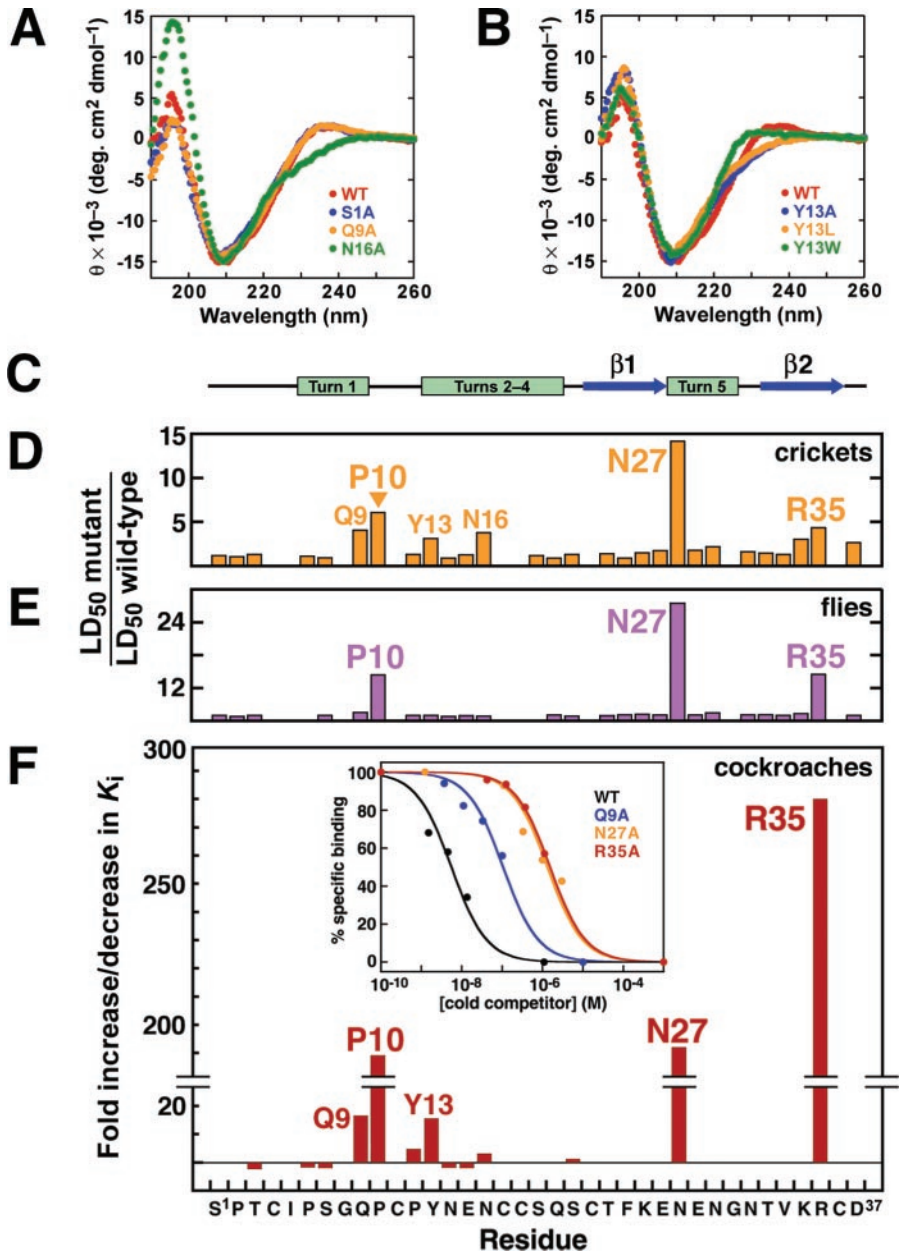

FIG. 1. **Mapping the insect-active epitope of ω-ACTX-Hv1a using alanine-scanning mutagenesis.** Comparison of the CD spectrum of WT recombinant ω-ACTX-Hv1a with S1A, Q9A, and N16A mutants (*A*) and Y13A, Y13L, and Y13W mutants (*B*). *C*, secondary structure of ω-ACTX-Hv1a as determined from NMR structural studies (2). *Sage boxes* represent β turns (labeled 1–5), whereas the two β strands that comprise the toxin's β hairpin are shown as *blue arrows*. *D*, histogram showing the -fold increase in LD_{50} in crickets (*Acheta domestica*) for each alanine mutation. *E*, histogram showing the-fold-increase in LD_{50} in flies (*Musca domestica*) for each alanine mutation. *F*, histogram showing the-fold-increase/decrease in K_i for binding of each alanine mutant to cockroach (*Periplaneta americana*) neuronal membranes. The inset shows representative binding curves for WT toxin and Q9A, N27A, and R35A mutants.

We were surprised to find that the presumed Tyr^{13} side chain signature was also absent in the N16A mutant (Fig. 1*A*). This suggests that the conformation of this mutant is perturbed in a manner that significantly alters the chemical environment of the Tyr^{13} side chain chromophore. Asn^{16} lies within a rare triple turn motif formed by three overlapping type I β turns (residues 13–16, 14–17, and 17–20) (2). Asn^{16} is found at the $i+2$ position of the second turn, where Asn and Asp are by far the most favored residues (18). In contrast, alanine is one of the least favored residues at this position in type I β turns (18). Thus, an N16A mutation might abrogate this β turn, thereby disrupting the entire set of interconnected β turns in the triple turn system and substantially altering the environment of the Tyr^{13} side chain. We therefore suspect that the small reduction in cricket toxicity observed for the N16A mutant (see below) is the result of a perturbation of the toxin structure in the region of the triple turn (residues 13–20). However, for all other alanine mutants, we can rule out the possibility that functional defects are caused by major structural perturbations.

Cricket Bioassays—The insecticidal potency of each mutant was initially examined by comparing its LD_{50} in a model orthopteran (house crickets) with that of WT recombinant toxin (Fig. 1*D*). Based on the reasoning described previously (11), we considered mutated residues to be functionally significant if the LD_{50} of the mutant toxin was more than 4-fold greater than that of WT toxin, potentially significant if the corresponding LD_{50} was 2–4-fold greater than that of WT toxin, or otherwise insignificant. We were surprised to find, based on these criteria, that only Gln^{9} and Pro^{10} were identified as functionally significant residues for activity against crickets (Fig. 1*D*), in addition to the β-hairpin residues Asn^{27} and Arg^{35} that were identified in our previous structure-activity relationship study (11). Residues Tyr^{13} and Asn^{16} were identified as potentially significant for cricket toxicity (Fig. 1*D*).

Fly Bioassays—We expanded the toxicity assays to include a model dipteran (house flies) for several reasons. First, dipterans are the most pernicious insects from a human and animal health perspective, being responsible for the transmission of malaria, filariasis, trypanosomiasis, leishmaniasis, and numerous arboviral diseases (4, 7). Thus, it was of interest to establish whether ω-ACTX-Hv1a might serve as a lead for

development of insecticides directed against dipteran vectors of human disease. Second, although some venomous animals such as cone snails are specialist predators, spiders are mostly generalists that prey on a wide range of invertebrates and sometimes small vertebrates. Thus, there would be selective advantage for spiders that evolved venoms capable of dealing with subtle variations in ion channel targets between different insects, in addition to the intraspecific complexity introduced by the high degree of differential splicing and editing of transcripts encoding channel subunits (19, 20). One evolutionary response to this problem seems to have been lineage-specific gene duplication events that created a suite of closely related paralogous toxins (21). However, an alternative possibility is that a single toxin encodes both a core pharmacophore that is crucial for interaction with the target plus additional residues that are critical contributors to channel binding in some insect species but not others. To address this latter possibility, we sought to examine whether the insect-active epitope of ω-ACTX-Hv1a was invariant between two highly divergent insect orders (*i.e.* Diptera and Orthoptera) or whether certain residues might be important for activity in one of these orders but not the other.

Finally, we were surprised that the cricket toxicity assays seemed to indicate that the insect-active epitope of ω-ACTX-Hv1a comprises only a few residues, thus raising the possibility that variations in toxin bioavailability/pharmacokinetics might be masking variations in channel-blocking activity of the mutant toxins. That is, in the LD_{50} assays, the activity of a toxin depends not only on its intrinsic affinity for the target channel but also on its *in vivo* stability and its ability to penetrate anatomical barriers. The latter point is crucial in that ω-ACTX-Hv1a targets the central nervous system of insects (4, 5), whereas most other spider toxins act presynaptically at insect neuromuscular junctions. Thus, a mutant toxin might have reduced activity not because of a reduced affinity for the target channel, but rather because of increased susceptibility to proteolysis or more limited access to the central nervous system. We anticipated that these potential problems would be less critical in the smaller house flies as they responded more rapidly than crickets to toxin injection, suggesting that anatomical barriers are less critical, and they were about 3-fold more sensitive to the toxin (LD_{50} = 86.5 ± 1.3 pmol/g) than crickets (LD_{50} = 269 ± 13 pmol/g).

Fig. 1*E* shows the insecticidal potency of each alanine mutant in house flies relative to the activity of the WT recombinant toxin. As for the cricket bioassays, residues Pro^{10}, Asn^{27}, and Arg^{35} were found to be functionally critical; each individual mutation caused a 10–20-fold reduction in LD_{50}. In contrast, Gln^9 and all residues identified as potentially significant in the cricket assays (Tyr^{13}, Asn^{16}, Asn^{29}, Lys^{34}, and Asp^{37}) seemed unimportant for activity against flies. An N27A,R35A double-mutant toxin (11) that carried mutations in two of the three residues most critical for insecticidal activity had a 60-fold higher LD_{50} in house flies than WT recombinant toxin (data not shown).

Competitive Binding Assays—We developed a competitive binding assay to study the interaction between ω-ACTX-Hv1a and its presumed calcium channel target in a manner not complicated by issues of pharmacokinetics and bioavailability. This assay measured the ability of cold ω-ACTX-Hv1a and alanine mutants thereof to displace the radiolabeled tracer ^{125}I-ω-ACTX-Hv1a from neuronal membranes prepared from the heads of adult cockroaches.

The assay was complicated by what seemed to be very high and inconsistent nonspecific binding of ^{125}I-ω-ACTX-Hv1a to the membrane preparation, a problem that could not be resolved through any modification of the assay conditions tested (*i.e.* using more or less toxin per binding reaction, more or less membrane preparation per binding reaction, additional washes, etc.). We presume this problem stems from two issues: 1) the low total number of ω-ACTX-Hv1a binding sites (B_{max} = 0.5–1.0 pmol/mg), consistent with the expected low density of voltage-gated calcium channels in excitable membranes (22); 2) the relatively low affinity of the tracer ($K_d \sim 5$ nM, see below). In contrast with ω-ACTX-Hv1a, the scorpion toxin Bj-xtrIT binds to cockroach neuronal membranes with K_d = 148 pM and B_{max} = 3 pmol/mg (23). The low receptor density and relatively low affinity of ω-ACTX-Hv1a for these receptors necessitated the use of large amounts of membrane for each binding reaction and a relatively high concentration (1–1.5 nM) of radioactive tracer. Nevertheless, in most cases, we obtained binding curves that did not appear disrupted by inconsistent background and which could be analyzed to yield reliable K_i values (see *inset* to Fig. 1*F* for examples of typical binding curves).

Scatchard analysis indicated that the K_d of the toxin for cockroach neuronal membranes was ~5 nM (n = 4). Although much lower than the affinity of Bj-xtrIT for cockroach neuronal membranes, the K_d is similar to that estimated for the scorpion toxin Lqh III under similar conditions (15). The K_d estimate was used with the Cheng-Prusoff equation under "Experimental Procedures" to calculate the fold increase/decrease in K_i for each mutant (Fig. 1*F*). Mutation to alanine of any of the three residues critical for toxicity against both crickets and flies (*i.e.* Pro^{10}, Asn^{27}, and Arg^{35}) reduced the K_i by more than 150-fold, with the R35A mutation causing a dramatic 280-fold reduction in binding affinity (Fig. 1*F*). The Q9A mutation, which reduced activity against crickets but not flies, caused a moderate 16-fold increase in K_i, as did the Y13A mutation (Fig. 1*F*). No other mutations significantly affected the binding of ω-ACTX-Hv1a to cockroach neuronal membranes. Thus, as observed in a previous study of scorpion α neurotoxins (24), there seems to be a good correspondence between the results of the binding and lethality assays. Differential bioavailability of mutants does not seem to be a major complicating factor in the LD_{50} assays, except perhaps for the R35A mutation, which was significantly more deleterious in binding studies than in lethality assays.

Chemical Features of the Toxin Pharmacophore—The alanine scanning mutagenesis studies indicated that Pro^{10}, Asn^{27}, and Arg^{35} are the key components of the toxin pharmacophore; Gln^9 and Tyr^{13} are of minor importance in orthopteroids (crickets and cockroaches) but unimportant in dipterans (see Fig. 1). By using a panel of non-alanine mutants, we showed previously that the γ-NH_2 group of Asn^{27} most probably donates a hydrogen bond to an acceptor on the target calcium channel, whereas the δ-guanido group of Arg^{35} most likely forms an ion pair with a carboxylate group on the channel (11). We decided to probe the chemical features of Gln^9 and Tyr^{13} to ascertain the nature of their interaction with orthopteroid calcium channels. CD analysis of toxins with mutations at Tyr^{13} (Fig. 1*B*) and Gln^9 (data not shown) indicated that their structures were similar to that of WT toxin.

A Y13F mutant was almost equipotent with native toxin in the cricket bioassay (Fig. 2*A*), which suggests that the hydroxyl group is relatively unimportant and that this residue mainly contacts the channel via hydrophobic interactions involving the aromatic ring. Consistent with this hypothesis, replacement of Tyr^{13} with leucine, a similarly sized hydrophobic, non-aromatic side chain, yielded a mutant toxin (Y13L) that had toxicity similar to that of the Y13F and native toxins. In contrast, replacement of Tyr^{13} with either a much smaller alanine residue (Y13A) or a significantly larger tryptophan residue (Y13W) caused a 3–4-fold reduction in LD_{50} (Fig. 2*A*). We conclude that

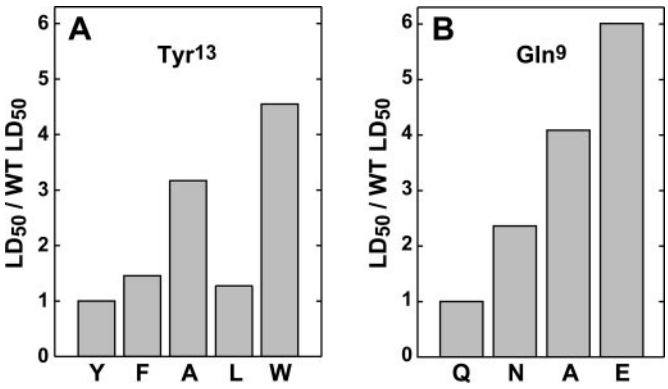

FIG. 2. **Probing chemical features of the toxin pharmacophore.** Histogram showing the-fold-increase in LD_{50} in crickets (*Acheta domestica*) for various point mutations at residues Tyr^{13} (*A*) and Gln^{9} (*B*). The *first bar* in each *histogram* corresponds to WT toxin.

Tyr^{13} makes contacts with a hydrophobic pocket in the channel that cannot be readily accessed by significantly smaller or larger hydrophobic sidechains at this position.

A Q9E mutant was about 50% less toxic to crickets than a Q9A mutant and had a 6-fold lower LD_{50} than WT toxin (Fig. 2*B*). It is impossible to determine from these data alone whether the loss of δ-NH_2 group, the introduction of a negative charge, or a combination of these factors is responsible for the large reduction in activity caused by the Q9E mutation. The data suggest, however, that the Gln^{9} side chain carbonyl group, which is retained in the Q9E mutant, does not make critical hydrogen bond interactions with the target channel. A Q9N mutation (2.4-fold reduction in LD_{50}) was significantly less deleterious than a Q9A mutation (4-fold reduction in LD_{50}) (Fig. 2*B*). We interpret these results to indicate that the δ-NH_2 of Gln^{9} makes hydrogen-bond interactions with acceptor groups on the channel and that this interaction can be retained to some degree when Gln^{9} is replaced by the slightly smaller Asn, in which the side chain is ~1.5 Å shorter.

Effect of ω-ACTX-Hv1a on Vertebrate Calcium Channels—We tested the effect of ω-ACTX-Hv1a and a functionally defective N27A,R35A double-mutant toxin on whole-cell calcium currents recorded from HEK cells that transiently expressed rat $Ca_v2.1$, $Ca_v2.2$, or $Ca_v1.2$ calcium channels. At a concentration of 10 μM, neither ω-ACTX-Hv1a nor the double-mutant toxin had any observable effect on calcium currents carried by these channels (data not shown). However, at a concentration of 30 μM, the WT toxin partially antagonized all three channel subtypes; the strongest inhibition was observed against $Ca_v1.2$ channels (Fig. 3). Remarkably, the inhibition of $Ca_v2.1$ and $Ca_v2.2$ currents was slightly enhanced in the double-mutant toxin, whereas the current block was marginally reduced for the $Ca_v1.2$ subtype. The fact that the moderate current block at this extremely high toxin concentration is not abrogated by the double mutation suggests that the weak inhibition of rat HVA calcium channels relies on structural determinants that are uniquely different from those involved in block of insect calcium channels.

DISCUSSION

Calcium Channels as Insecticide Targets—Peptidic calcium channel blockers have been isolated from the venoms of numerous spiders, including plectoxin II from *Plectreurys tristes*, CSTX-1 from the subtropical wandering spider *Cupiennius salei*, several families of ω-agatoxins from the American funnel-web spider *Agelenopsis aperta*, and two families of ω-atracotoxins from various species of Australian funnel-web spiders (genera *Atrax* and *Hadronyche*) (7). The evolution of calcium channel blockers in spider venoms as part of a mechanism for incapacitating envenomated prey is not surprising because voltage-gated calcium channels (VGCCs) play critical roles in modulating synaptic transmission in insects. The essential role of insect VGCCs is highlighted by the fact that the *D. melanogaster* genome appears to encodes pore-forming α_1-subunits for only one Ca_v1 family member (*Dmca1D*) and one Ca_v2 family member (*Dmca1A/cacophony*) (25), and severe loss-of-function mutations in either of these genes is embryonic lethal (26–28).

Despite the fact that insect VGCCs seem to be excellent insecticide targets, as first suggested almost a decade ago (29), no commercial insecticides have ever been directed against these channels. The limited phyletic specificity of the ω-agatoxins may have promoted the misconception that insect VGCCs could not be *selectively* targeted. However, this view is at odds with the fact that insect and vertebrate VGCCs are pharmacologically distinct, with different susceptibilities to a range of peptide toxins and chemical agents (30). Our recent isolation of two families of highly insect-selective ω-atracotoxins (4, 10) demonstrates that phyletically specific targeting of insect VGCCs is indeed possible. This is further exemplified in the current study, where we demonstrated that ω-ACTX-Hv1a is lethal to a range of insect species but inactive against heterologously expressed rat HVA VGCCs even at concentrations as high as 10 μM.

The Insect-specific Pharmacophore of ω-ACTX-Hv1a—The specificity of ω-ACTX-Hv1a for insect VGCCs makes it an excellent lead for the development of insecticides directed against insect calcium channels. In this study, we mapped the pharmacophore of ω-ACTX-Hv1a to provide a template for rational design of such insecticides. The cockroach neuronal membrane binding assays and the two sets of insect bioassays all identified three functionally critical residues (Pro^{10}, Asn^{27}, and Arg^{35}; see Fig. 1, *D–F*) that we presume correspond to the primary VGCC-binding epitope of the toxin. It is remarkable that these residues, although well separated in the amino acid sequence, form a spatially contiguous epitope when mapped onto the three-dimensional structure of ω-ACTX-Hv1a (Fig. 4*A*). Arg^{35} is positioned at the center of this binding "hot spot," flanked by Pro^{10} and Asn^{27}.

Arg is one of the most highly enriched residues at protein-protein interfaces (31), and Arg^{35} seems to be the most critical residue for binding of ω-ACTX-Hv1a to cockroach VGCCs; mutation of Arg^{35} to Ala caused a 280-fold reduction in K_i (see Fig. 1*F*), which corresponds to a change in the free energy of binding ($\Delta\Delta G_{bind}$) of 3.3 kcal/mol. Mutation of the flanking Pro^{10} and Asn^{27} residues to Ala caused a smaller ~180-fold reduction in K_i, corresponding to a $\Delta\Delta G_{bind}$ of ~3.1 kcal/mol. Gln^{9} and Tyr^{13} seem to be of minor importance for binding of the toxin to orthopteroid VGCCs, with mutation of these residues to Ala giving a $\Delta\Delta G_{bind}$ of only ~1.6 kcal/mol. Gln^{9} is contiguous with the core pharmacophore, whereas the Tyr^{13} side chain is situated ~12 Å from the binding hot spot (Fig. 4*A*). These residues do not seem to be important for binding of the toxin to dipteran VGCCs.

Sequencing of venom peptides (1, 3) and analysis of venom-gland cDNA libraries (4, 21) has revealed that each species of Australian funnel-web spider typically expresses a complement of 3–6 ω-ACTX-Hv1a homologs in its venom. Despite significant intra- and interspecific variations in the sequences of these homologs, the five pharmacophore residues (Gln^{9}, Pro^{10}, Tyr^{13}, Asn^{27}, and Arg^{35}) are identical in all ω-ACTX-1 orthologs that have been sequenced to date (see Fig. 3*A* in Ref. 4 for an alignment of 11 representative ω-ACTX-1 sequences). Thus, the data currently available seem to indicate that the pharmacophore of ω-ACXT-Hv1a has been universally conserved in this family of spiders.

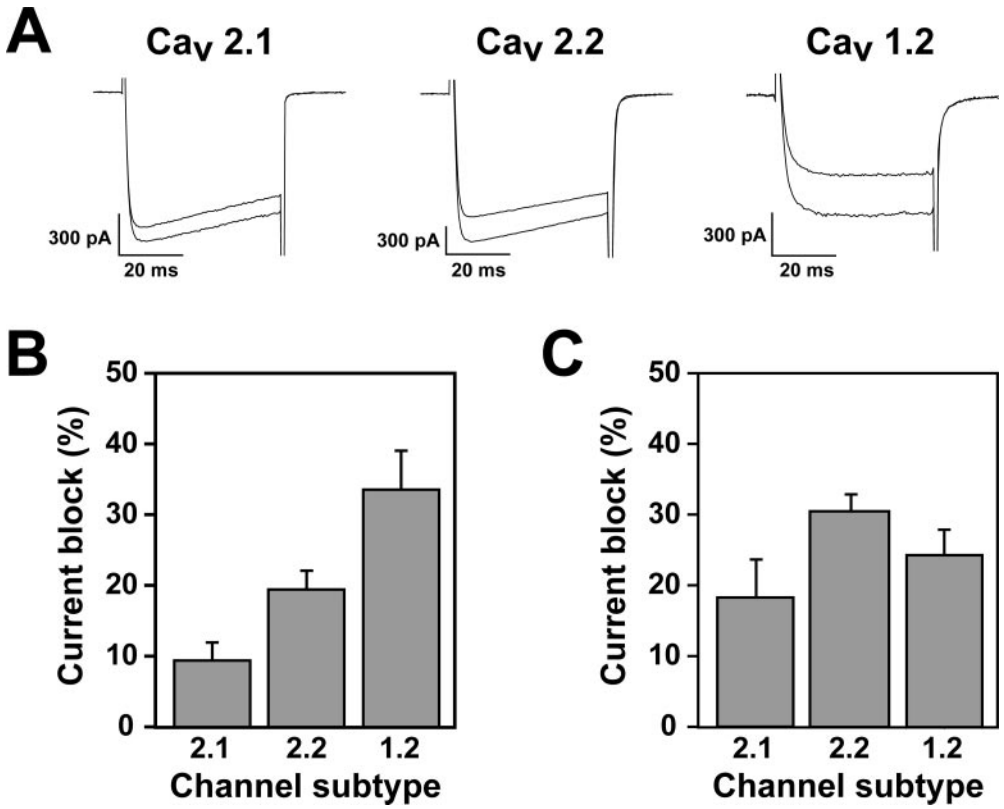

FIG. 3. **Effect of ω-ACTX-Hv1a on rat HVA calcium channels.** *A*, whole-cell calcium current recordings showing the effect of 30 μM wild-type ω-ACTX-Hv1a on currents carried by rat HVA calcium channels transiently expressed in HEK cells. *B* and *C*, extent of current blockage for each channel subtype caused by either 30 μM ω-ACTX-Hv1a (*B*) or a functionally defective double mutant toxin carrying N27A and R35A mutations (*C*). Toxins were applied to transfected HEK cells in 20 mM Ba^{2+} recording solution at a holding potential of −100 mV. Test currents were elicited by voltage stepping to +20 mV. Data are the average of recordings from six cells.

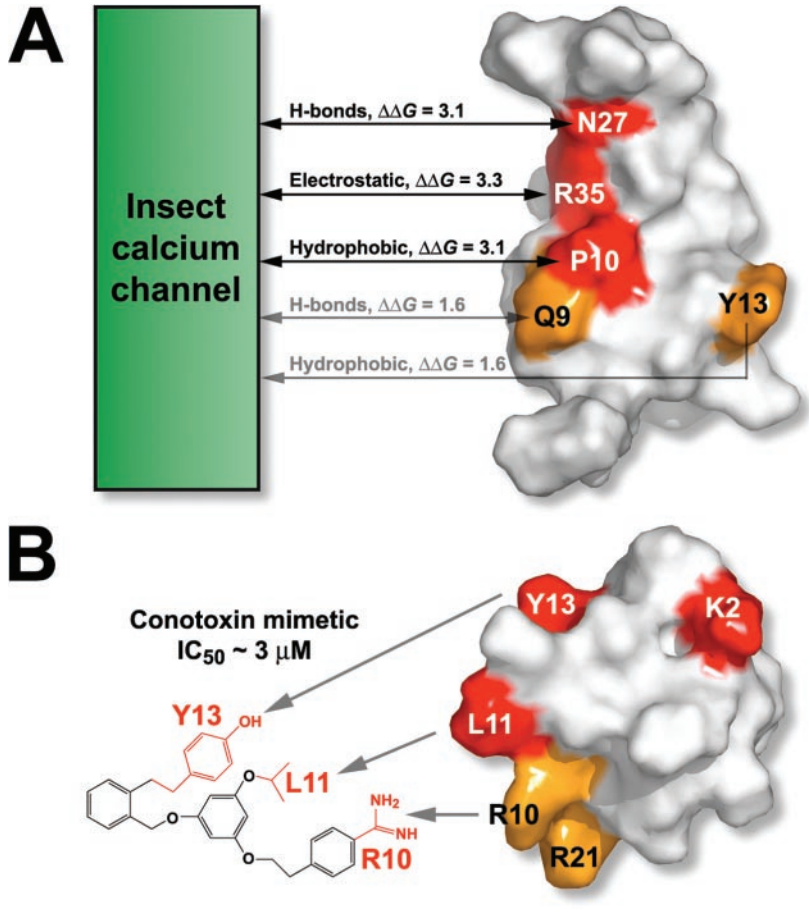

FIG. 4. **The pharmacophore of ω-ACTX-Hv1a.** *A*, molecular surface of ω-ACTX-Hv1a (Protein Data Base file 1AXH; (2)) with core pharmacophore residues (Pro^{10}, Asn^{27}, and Arg^{35}; $\Delta\Delta G_{bind}$ > 2.5 kcal/mol) shown in *red*. Residues drawn in *orange* (Gln^{9} and Tyr^{13}; $\Delta\Delta G_{bind}$ ~1.6 kcal/mol) are of minor importance for binding to orthopteroid VGCCs but seem to be unimportant for interaction of the toxin with dipteran calcium channels. Proposed molecular interactions with orthopteroid calcium channels are summarized above each *double-headed arrow*. $\Delta\Delta G_{bind}$ values, which indicate the loss of binding energy (in kilocalories per mole) resulting from mutation of the indicated residue to Ala, were calculated using the equation $\Delta\Delta G_{bind} = RT\ln(\text{wild-type } K_i/\text{mutant } K_i)$. *B*, molecular surface of ω-conotoxin MVIIA (Protein Data Base file 1OMG; (48)) with key pharmacophore residues shown in *red* ($\Delta\Delta G_{bind}$ > 2.5 kcal/mol) and *orange* ($\Delta\Delta G_{bind}$ = 1.8–2.2 kcal/mol). $\Delta\Delta G_{bind}$ values resulting from mutation of the indicated residues to Ala were calculated from IC_{50} values reported in Ref. 36. The illustrated mimetic of ω-conotoxin MVIIA, which was rationally designed to mimic three key pharmacophore residues (Arg^{10}, Leu^{11}, and Tyr^{13}), had an IC_{50} of ~3 μM against rat Ca_v 2.2 channels (46). Molecular surfaces were drawn using PyMOL (49).

Comparison of the ω-ACTX-Hv1a Pharmacophore with VGCC-binding Epitopes on Other Toxins—As far as we are aware, the only other toxin VGCC-binding epitopes that have been mapped in detail are those on the functionally homologous cone snail toxins ω-conotoxin GVIA (32–34) and ω-conotoxin MVIIA (35, 36). Extensive mutagenesis of these ω-conotoxins, which selectively block HVA currents carried by vertebrate Ca_V 2.2 (N-type) VGCCs, revealed a more extensive, discontinuous pharmacophore than we elucidated in this study for ω-ACTX-Hv1a (see Ref. 37 for a review). That is, although the three residues that form the core pharmacophore of ω-ACTX-Hv1a (*i.e.* Pro^{10}, Asn^{27}, and Arg^{35}) are spatially contiguous (Fig. 4*A*), the three key residues in the pharmacophore of ω-conotoxin MVIIA (*i.e.* Lys^2, Leu^{11}, and Tyr^{13}) are discontinuous and their sidechains are separated from one another (as measured using the βC atoms) by 7–15 Å (Fig. 4*B*). Moreover, in contrast with ω-ACTX-Hv1a, scanning mutagenesis of both ω-conotoxin GVIA and ω-conotoxin MVIIA revealed numerous residues that make minor contributions to channel binding ($\Delta\Delta G_{bind} < 1.6$ kcal/mol) (37).

The ω-ACTX-Hv1a pharmacophore cannot be superimposed on a subset of the key VGCC-binding residues in either of the ω-conotoxins, consistent with our observation that physiological concentrations of ω-ACTX-Hv1a do not block HVA currents carried by heterologously expressed rat Ca_V 2.2 channels. Lys^2 and Tyr^{13} are the two most critical residues for block of vertebrate Ca_V 2.2 channels by the ω-conotoxins, but these residue types are not even present in the primary ω-ACTX-Hv1a pharmacophore. We conclude that the ω-conotoxins and ω-ACTX-Hv1a make markedly different types of interactions with their cognate calcium channel targets.

Using ω-ACTX-Hv1a as a Template for Mimetic Design—Heterologous expression of the cognate calcium channel target of ω-ACTX-Hv1a in an easily manipulated cell line could be exploited to develop high throughput screens of chemical libraries to uncover lead chemical insecticides based on the mode of action of ω-ACTX-Hv1a. Although high-throughout screening has become a dominant paradigm in the pharmaceutical industry, it typically produces few viable leads; despite the impressive size of many compound libraries, they are often limited in pharmacophore diversity (38). Indeed, although chemical libraries have become a critical part of the lead identification process in insecticide and pharmaceutical discovery, about two-thirds of all 1031 newly approved drugs in the period 1983–2002 were either natural products or compounds derived from natural products (39). Many of the most successful insecticidal compounds have also been derived from natural products, including the pyrethroids, spinosads, avermectins, and *Bacillus thuringiensis* δ-endotoxins (40). Thus, a potentially rewarding alternative to high throughput screens based on heterologous expression of the target of ω-ACTX-Hv1a is rational design of insecticides based on the toxin's pharmacophore.

In recent years, there have been several impressive examples of rational design of small molecules based on mimicry of protein-binding epitopes, a process we refer to as "pharmacophore cloning" (41, 42). For example, Genentech recently designed small molecules that mimic the complicated but spatially contiguous LFA-1 binding epitope on intercellular adhesion molecule-1 (43). More relevant to the current discussion are three recent studies in which attempts were made to clone the pharmacophores of peptide toxins that block vertebrate calcium or potassium channels (44–46). In the most successful study, the pharmacophore of ω-conotoxin MVIIA was mimicked by decorating an alkylphenyl backbone with chemical groups corresponding to three key functional residues (Arg^{10}, Leu^{11}, and Tyr^{13}) identified in an alanine scan (Fig. 4*B*). Even though, as discussed above, the pharmacophore of ω-conotoxin MVIIA is discontinuous and other residues such as Lys^2 are known to be involved in the toxin-channel interaction, the rationally designed nonpeptide mimetics had IC_{50} values of ~3 μM against human N-type VGCCs (46). Although native ω-conotoxin MVIIA binds these channels with considerably higher subnanomolar affinity (35–37), the rationally designed mimetics nevertheless have sufficient affinity to make them desirable leads for further optimization as antinociceptive agents (46).

As far as we are aware, there is no precedent for synthetic imitation of the pharmacophore of an insecticidal peptide toxin with the aim of developing an insecticide. The primary reason for this is presumably lack of suitable design templates. To date, besides ω-ACTX-Hv1a, the pharmacophores have been mapped for only three other insect-selective toxins: J-ACTX-Hv1c from the Australian funnel-web spider *Hadronyche versuta* (47) and insecticidal neurotoxins from the scorpions *Leiurus quinquestriatus hebraeus* (LqhαIT) (24) and *Buthotus judaicus* (Bj-xtrIT) (23). ω-ACTX-Hv1a most likely presents a best case scenario for rational insecticide design because this peptide is about half the size of the scorpion toxins, and its pharmacophore is much less complicated. The core ω-ACTX-Hv1a pharmacophore (*i.e.* residues Pro^{10}, Asn^{27}, and Arg^{35}) corresponds to a contiguous surface area of ~200 $Å^2$, which approximates the typical solvent-accessible surface area (150–500 $Å^2$) of a small drug (41). In contrast, the pharmacophore of Bj-xtrIT encompasses a discontinuous surface area of 1405 $Å^2$ (23), which represents a much more difficult template for design of nonpeptide mimetics.

It is hoped that the mapped pharmacophore of ω-ACTX-Hv1a will facilitate development of a new rational design paradigm in insecticide discovery. However, a key question that remains to be addressed is whether a rationally designed nonpeptide mimetic can maintain the remarkable and highly desirable phyletic specificity of the parent peptide toxin. Residues deemed not to be functionally important according to insect functional studies might nevertheless provide a steric impediment to binding to the vertebrate counterpart of the targeted insect channel. Failure to consider this might lead to phyletically indiscriminate mimetics with an unacceptable toxicological profile.

Acknowledgments—We thank Dr. Zheng-yu Peng for access to CD instrumentation. Electrospray mass spectral data were collected by Dr. John Lesyk at the University of Massachusetts Proteomic Mass Spectrometry Lab, which is supported, in part, by the National Science Foundation.

REFERENCES

1. Atkinson, R. K., Howden, M. E. H., Tyler, M. I., and Vonarx, E. J. (June 9, 1998) U. S. Patent 5,763,568
2. Fletcher, J. I., Smith, R., O'Donoghue, S. I., Nilges, M., Connor, M., Howden, M. E. H., Christie, M. J., and King, G. F. (1997) *Nat. Struct. Biol.* **4,** 559–566
3. Wang, X.-H., Smith, R., Fletcher, J. I., Wilson, H., Wood, C. J., Howden, M. E. H., and King, G. F. (1999) *Eur. J. Biochem.* **264,** 488–494
4. Tedford, H. W., Sollod, B. L., Maggio, F., and King, G. F. (2004) *Toxicon* **43,** 601–618
5. Bloomquist, J. R. (2003) *Invertebr. Neurosci.* **5,** 45–50
6. Brogdon, W. G., and McAllister, J. C. (1998) *Emerg. Infect. Dis.* **4,** 605–613
7. Maggio, F., Sollod, B. L., Tedford, H. W., and King, G. F. (2004) in *Comprehensive Molecular Insect Science* (Gilbert, L. I., Iatrou, K., and Gill, S., eds), Elsevier, in press
8. Olivera, B. M., Miljanich, G. P., Ramachandran, J., and Adams, M. E. (1994) *Annu. Rev. Biochem.* **63,** 823–867
9. de Weille, J. R., Schweitz, H., Maes, P., Tartar, A., and Lazdunski, M. (1991) *Proc. Natl. Acad. Sci. U. S. A.* **88,** 2437–2440
10. King, G. F., Tedford, H. W., and Maggio, F. (2002) *J. Toxicol. Toxin Rev.* **21,** 359–389
11. Tedford, H. W., Fletcher, J. I., and King, G. F. (2001) *J. Biol. Chem.* **276,** 26568–26576
12. Maggio, F., and King, G. F. (2002) *Toxicon* **40,** 1355–1361
13. Eitan, M., Fowler, E., Herrmann, R., Duval, A., Pelhate, M., and Zlotkin, E. (1990) *Biochemistry* **29,** 5941–5947
14. Favreau, P., Gilles, N., Lamthanh, H., Bournaud, R., Shimahara, T., Bouet, F., Laboute, P., Letourneux, Y., Menez, A., Molgo, J., and Le Gall, F. (2001) *Biochemistry* **40,** 14567–14575

15. Krimm, I., Gilles, N., Sautiere, P., Stankiewicz, M., Pelhate, M., Gordon, D., and Lancelin, J. M. (1999) *J. Mol. Biol.* **285,** 1749–1763
16. Cheng, Y., and Prusoff, W. H. (1973) *Biochem. Pharmacol.* **22,** 3099–3108
17. Jarvis, S. E., and Zamponi, G. W. (2001) *J. Neurosci.* **21,** 2939–2948
18. Hutchinson, E. G., and Thornton, J. M. (1994) *Protein Sci.* **3,** 2207–2216
19. Hoopengardner, B., Bhalla, T., Staber, C., and Reenan, R. (2003) *Science* **301,** 832–836
20. Zamponi, G. W., and McCleskey, E. W. (2004) *Neuron* **41,** 3–4
21. Sollod, B. L., Wilson, D., Zhaxybayeva, O., Gogarten, J. P., Drinkwater, R., and King, G. F. (2004) *Peptides*, in press
22. Hille, B. (2001) *Ion Channels of Excitable Membranes*, 3rd ed., Sinauer Associates, Sunderland, MA
23. Cohen, L., Karbat, I., Gilles, N., Froy, O., Corzo, G., Angelovici, R., Gordon, D., and Gurevitz, M. (2004) *J. Biol. Chem.* **279,** 8206–8211
24. Zilberberg, N., Froy, O., Loret, E., Cestèle, S., Arad, D., Gordon, D., and Gurevitz, M. (1997) *J. Biol. Chem.* **272,** 14810–14816
25. Littleton, J. T., and Ganetzky, B. (2000) *Neuron* **26,** 35–43
26. Eberl, D. F., Ren, D., Feng, G., Lorenz, L. J., Vactor, D. V., and Hall, L. M. (1998) *Genetics* **148,** 1159–1169
27. Smith, L. A., Peixoto, A. A., Kramer, E. M., Villella, A., and Hall, J. C. (1998) *Genetics* **149,** 1407–1426
28. Kawasaki, F., Collins, S. C., and Ordway, R. W. (2002) *J. Neurosci.* **22,** 5856–5864
29. Hall, L. M., Ren, D., Feng, G., Eberl, D. F., Dubald, M., Yang, M., Hannan, F., Kousky, C. T., and Zheng, W. (1995) in *Molecular Action of Insecticides on Ion Channels* (Clark, J. M., ed), pp. 162–172, American Chemical Society, Washington, DC
30. Wicher, D., and Penzlin, H. (1997) *J. Neurophysiol.* **77,** 186–199
31. Bogan, A. A., and Thorn, K. S. (1998) *J. Mol. Biol.* **280,** 1–9
32. Kim, J. I., Takahashi, M., Ogura, A., Kohno, T., Kudo, Y., and Sato, K. (1994) *J. Biol. Chem.* **269,** 23876–23878
33. Lew, M. J., Flinn, J. P., Pallaghy, P. K., Murphy, R., Whorlow, S. L., Wright, C. E., Norton, R. S., and Angus, J. A. (1997) *J. Biol. Chem.* **272,** 12014–12023
34. Flinn, J. P., Pallaghy, P. K., Lew, M. J., Murphy, R., Angus, J. A., and Norton, R. S. (1999) *Eur. J. Biochem.* **262,** 447–455
35. Kim, J. I., Takahashi, M., Ohtake, A., Wakamiya, A., and Sato, K. (1995) *Biochem. Biophys. Res. Commun.* **206,** 449–454
36. Nadasdi, L., Yamashiro, D., Chung, D., Tarczy-Hornoch, K., Adriaenssens, P., and Ramachandran, J. (1995) *Biochemistry* **34,** 8076–8081
37. Nielsen, K. J., Schroeder, T., and Lewis, R. (2000) *J. Mol. Recognit.* **13,** 55–70
38. Muegge, I. (2002) *Chem. Eur. J.* **8,** 1976–1981
39. Newman, D. J., Cragg, G. M., and Snader, K. M. (2003) *J. Nat. Prod.* **66,** 1022–1037
40. Copping, L. G., and Menn, J. J. (2000) *Pest. Manag. Sci.* **56,** 651–676
41. Gadek, T. R., and Nicholas, J. B. (2003) *Biochem. Pharmacol.* **65,** 1–8
42. Arkin, M. R., and Wells, J. A. (2004) *Nat. Rev. Drug. Discov.* **3,** 301–317
43. Gadek, T. R., Burdick, D. J., McDowell, R. S., Stanley, M. S., Marsters, J. C., Jr., Paris, K. J., Oare, D. A., Reynolds, M. E., Ladner, C., Zioncheck, K. A., Lee, W. P., Gribling, P., Dennis, M. S., Skelton, N. J., Tumas, D. B., Clark, K. R., Keating, S. M., Beresini, M. H., Tilley, J. W., Presta, L. G., and Bodary, S. C. (2002) *Science* **295,** 1086–1089
44. Baell, J. B., Forsyth, S. A., Gable, R. W., Norton, R. S., and Mulder, R. J. (2001) *J. Comput. Aided Mol. Des.* **15,** 1119–1136
45. Baell, J. B., Harvey, A. J., and Norton, R. S. (2002) *J. Comput. Aided Mol. Des.* **16,** 245–262
46. Menzler, S., Bikker, J. A., Suman-Chauhan, N., and Horwell, D. C. (2000) *Bioorg. Med. Chem. Lett.* **10,** 345–347
47. Maggio, F., and King, G. F. (2002) *J. Biol. Chem.* **277,** 22806–22813
48. Kohno, T., Kim, J. I., Kobayashi, K., Kodera, Y., Maeda, T., and Sato, K. (1995) *Biochemistry* **34,** 10256–10265
49. DeLano, W. L. (2002) *The PyMOL Molecular Graphics System*, DeLano Scientific, San Carlos, CA

Scanning Mutagenesis of ω-Atracotoxin-Hv1a Reveals a Spatially Restricted Epitope That Confers Selective Activity against Insect Calcium Channels

Hugo W. Tedford, Nicolas Gilles, André Ménez, Clinton J. Doering, Gerald W. Zamponi and Glenn F. King

J. Biol. Chem. 2004, 279:44133-44140.
doi: 10.1074/jbc.M404006200 originally published online August 11, 2004
